

Reduction in the electronic band gap of titanium oxide nanotubes

Zejian Liu^a, Qi Zhang^a, Lu-Chang Qin^{a,b,*}

^a *W.M. Keck Laboratory for Atomic Imaging and Manipulation, Department of Physics and Astronomy, University of North Carolina at Chapel Hill, Campus Box 3255, Chapel Hill, NC 27599-3255, USA*

^b *Curriculum in Applied and Materials Sciences, University of North Carolina at Chapel Hill, Chapel Hill, NC 27599-3255, USA*

Received 30 October 2004; received in revised form 19 July 2006; accepted 14 September 2006 by S.G. Louie
Available online 26 October 2006

Abstract

The structural and electronic properties of individual titanium oxide nanotubes have been studied using both empirical and *ab initio* calculations. Two different types of titanium oxide nanotubes (A-nanotube and B-nanotube) have been constructed and energy-minimized by molecular mechanics calculations. We found that the A-nanotubes are energetically more favorable than the B-nanotubes. The electronic band structure of the titanium oxide nanotubes was also calculated with respect to the tubule diameter and the tubule type using the *ab initio* method. The band gap of the A-nanotube was reduced by up to 60% as the tubule diameter decreases from 1.2 nm to 0.5 nm.

© 2006 Elsevier Ltd. All rights reserved.

PACS: 71.15.Nc; 73.63.Fg; 78.67.Ch

Keywords: A. TiO₂; A. Nanotube; D. Band gap

1. Introduction

Since the discovery of carbon nanotubes [1], there has been an intense interest in synthesizing one-dimensional tubular structures at the nanoscale, which show novel chemical and physical properties different from their bulk forms. According to the origin of their atomic formation, nanotubes can be classified into two categories: (a) nanotubes formed by wrapping up along a chosen tubule axis of layered materials such as graphite and boron nitride [1,2] and (b) nanotubes based on the d-metal oxides such as SnO₂, SiO₂, Al₂O₃, V₂O₅, and TiO₂ [3–7]. Depending on the synthesis method, the diameter of nanotubes can vary from sub-nanometer to tens of nanometers. Among the nanotubes synthesized so far in category (b), titanium oxide (TiO₂) nanotubes have aroused much interest due to their potential applications in photocatalysis [8,9], high efficient solar cells [10], biological coatings [11], and sensors [12].

TiO₂ exists in three different crystalline structures: anatase, rutile and brookite. The anatase structure has attracted much attention over the last few decades for its technological applications. TiO₂ in the anatase phase exhibits a high photocatalytic activity, which is promising for the envisaged applications in such areas as environmental purification, decomposition of carbonic acid gas, and generation of hydrogen gas by decomposing water with solar energy [13–15]. However, due to the large band gap of TiO₂ (about 3.2 eV in the anatase phase [16]), titania powders can only absorb ultraviolet light in the solar spectrum, which occupies less than 10% of the total solar energy [17]. To make a full use of the solar energy and to increase the photocatalytic efficiency, it is necessary to reduce the band gap of TiO₂ into the range in which visible light could be absorbed. TiO₂ nanotubes of the anatase form are a promising structure to have a smaller band gap than the bulk powders. Furthermore, TiO₂ nanotubes possess large surface area which can further increase the photocatalytic efficiency.

In this Letter, we propose and examine two model structures of TiO₂ nanotubes of the anatase form, which are energy-minimized by employing molecular mechanics calculations. Both the structural and electronic properties of the TiO₂ nanotubes have been studied in detail, with the electronic

* Corresponding author at: W.M. Keck Laboratory for Atomic Imaging and Manipulation, Department of Physics and Astronomy, University of North Carolina at Chapel Hill, Campus Box 3255, Chapel Hill, NC 27599-3255, USA. Tel.: +1 919 843 3575; fax: +1 919 962 0480.

E-mail address: lcqin@physics.unc.edu (L.-C. Qin).

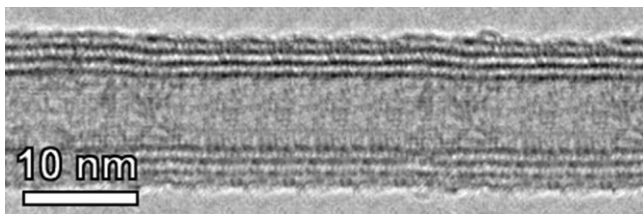


Fig. 1. High-resolution transmission electron microscopy image of a TiO₂ nanotube consisting of four layers.

properties calculated by performing density functional theory (DFT) calculations in order to obtain their band gaps.

2. Structure models of TiO₂ nanotubes

TiO₂ nanotubes of the anatase form can now be produced routinely in the laboratory by a hydrothermal method [18]. Fig. 1 shows a high-resolution transmission electron microscope image of a typical TiO₂ nanotube that consists of four walls as indicated by the four sets of dark line pairs across the hollow core.

The electronic band gap of TiO₂ nanotubes increases monotonically with the tubule diameter. However, when the diameter is large, the band gap is not sensitive to the diameter as the steric deformation is small compared to the structure of the bulk TiO₂ crystals. We therefore only constructed model structures of small diameters in the present study.

Since *ab initio* calculations are very computationally intensive for structural optimization, for large systems that consist of thousands of atoms, classical methods such as molecular mechanics simulations are used for structural relaxation in this study. In the following studies of TiO₂ nanotubes, we apply molecular mechanics based calculations to obtain the optimized TiO₂ nanotube structure, while the electronic band structures are obtained by performing DFT calculations.

In the molecular mechanics simulations, the interactions between the atoms are modeled by a universal force field (UFF), which applies to the anatase crystals very well [19]. The functional forms of the force field are expressed as follows:

$$\begin{aligned}
 E_{\text{tot}} = & \sum_b K_2(b - b_0)^2 + \sum_{\theta} H_2(\theta - \theta_0)^2 \\
 & + \sum_{\phi} \sum_{j=1}^3 V_j(1 - 2\cos(\phi - \phi_j^0)) \\
 & + \sum_{i>j} \left(\frac{A_{ij}}{r_{ij}^{12}} - \frac{B_{ij}}{r_{ij}^6} \right) + \sum_{i>j} B \frac{q_i q_j}{r_{ij}} \quad (1)
 \end{aligned}$$

where $b - b_0$ stands for the bond stretching, $\theta - \theta_0$ stands for the angle bending, the torsion angle ϕ is expressed in the three-term Fourier cosine expansions, r_{ij} are the distance between atoms i and j that have charges of q_i and q_j , respectively, K_2 , H_2 , V_j and B are coefficients in the corresponding energy-functional terms, and the van der Waals interactions are described by the Lennard–Jones potential with coefficients A_{ij} and B_{ij} , respectively. Structural optimization was then performed in the

conjugate gradient scheme with a convergence of 1×10^{-7} for the energetic calculations. The DFT-based *ab initio* calculations were implemented in the commercial package DMol3 to obtain the electronic band structure of the TiO₂ nanotubes using a kinetic energy cut off of 300 eV. The exchange–correlation potential energy terms are evaluated in the local density approximation (LDA) schemes with the Perdew–Wang parameterization [20–22]. A calculation basis set (using 100 k -points) consisting of double numeric functions as well as polarization functions were employed in the calculations. Since the TiO₂ nanotube model structures are periodic in the tubule axis direction, the band structure calculations were implemented by building a tetragonal super-unit cell, with the lattice parameter a' being much larger than the diameter of the TiO₂ nanotube and the other lattice parameter c' the periodicity of the nanotube. By doing so, the edge effect in modeling the nanotube structure has been reduced to minimal.

A single-layer TiO₂ nanotube can be formed by wrapping up a (101) layer of TiO₂ of the anatase structure [23] along either the $[\bar{1}01]$ direction or the $[010]$ direction. Since the single-layer structure of anatase is a high-energy state and has to relax, deformation would usually take place leading to a tubular structure. In either of these two configurations, due to the energy minimization, the dangling bonds will reconstruct to form a seamless tubular structure. Since anatase has a tetragonal Bravais lattice, in the present investigation, two types of TiO₂ nanotubes have been constructed as shown in Fig. 2: the TiO₂ nanotubes with tubule axis in the $[\bar{1}01]$ direction (A-nanotube) and the TiO₂ nanotubes with tubule axis in the $[010]$ direction (B-nanotube). Fig. 2(a) and (b) show the relaxed structure of an A-nanotube in side view and cross-sectional view, respectively, and Fig. 2(c) and (d) show the relaxed structure in projection of a B-nanotube.

The displayed model structures of the TiO₂ nanotubes were energy-minimized by molecular mechanics simulations with the UFF force field. From the molecular mechanics simulations, we found that the total energy of the TiO₂ nanotubes depended on both their diameter and their type (A or B). Fig. 3 shows the relationship between the total energy and the diameter for the A-nanotube and B-nanotube, respectively. The total energy of the TiO₂ nanotubes of both types is inversely proportional to the tubule diameter, largely due to the steric strains introduced to the structure when the diameter is small. In particular, for the A-nanotube, the total energy increases drastically as the tubule diameter is reduced to about 1 nm. In addition, we have noticed that the A-nanotube is energetically more favorable than the B-nanotube. For example, for the TiO₂ nanotubes with diameters of approximately 1.6 nm, the total energy of the B-nanotube is higher than that of the A-nanotube by 0.15 eV/TiO₂ unit. Moreover, due to the difference in unit cell dimensions c and a ($a = b = 0.3783$ nm, $c = 0.9502$ nm) of the tetragonal Bravais lattice [23], the minimum diameters of the A-nanotube and the B-nanotube are different. The diameter of the B-nanotubes can not go below 1 nm, but the diameter of the A-nanotubes can go down to 0.5 nm while the nanotube still retains a concentric structure as described above.

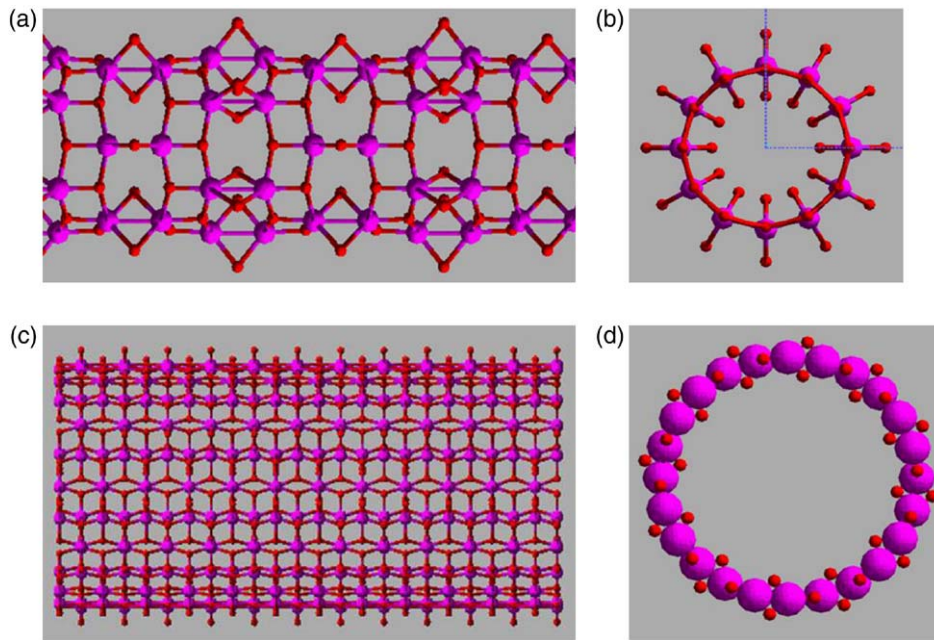


Fig. 2. (a) Side view of a TiO_2 A-nanotube formed by rolling up one (101) optimized layer along $[\bar{1}01]$ direction. The periodicity along tube axis $[\bar{1}01]$ is approximately 1.04 nm, which is slightly larger than that of the anatase structure ($c = 0.9486$ nm). (b) Cross-sectional view of the TiO_2 A-nanotube. (c) Side view of a TiO_2 B-nanotube formed by rolling up the geometry-optimized (101) layer along $[100]$ direction. The periodicity in the tubule axis direction $[100]$ is approximately 0.371 nm, which is smaller than that of the anatase structure ($a = 0.3776$ nm). (d) Cross-sectional view of the TiO_2 B-nanotube.

3. Electronic band structure of TiO_2 nanotubes

Fig. 4(a) and (b) show the electronic band structure of the A- and B-nanotubes, respectively. It is interesting to note that the A-nanotube of diameter 0.8 nm has a band gap of 1.90 eV, whereas the B-nanotube of diameter 1.69 nm has a band gap of 2.44 eV. More interestingly, the electronic band structure of the B-nanotube is different from that of the A-nanotube. The A-nanotube has a direct band gap at $k = 0$ while the B-nanotube has an indirect band gap, which occurs between $k = 0$ and $k = 1/3c$ in the reciprocal space, where k is the wave vector. As the diameter of TiO_2 nanotubes changes, the electronic band gap changes accordingly.

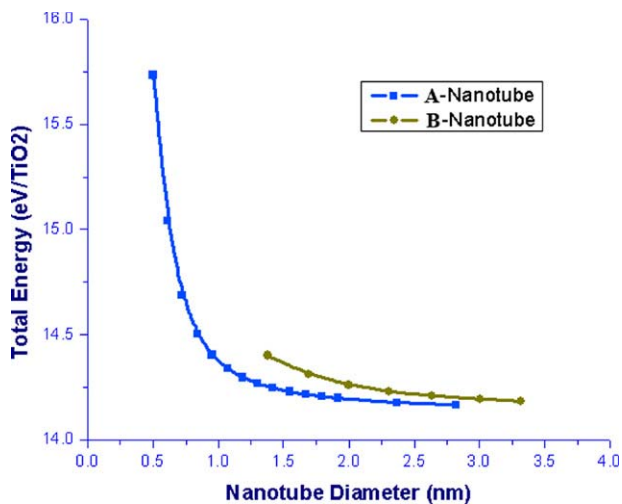


Fig. 3. Relationship between the total energy and the tubule diameter of (a) TiO_2 A-nanotubes and (b) TiO_2 B-nanotubes. The total energy for an A-nanotube is lower than the B-nanotube of the same diameter.

Fig. 5 shows that the band gap for both types of TiO_2 nanotube decreases as the nanotube diameter decreases. As a

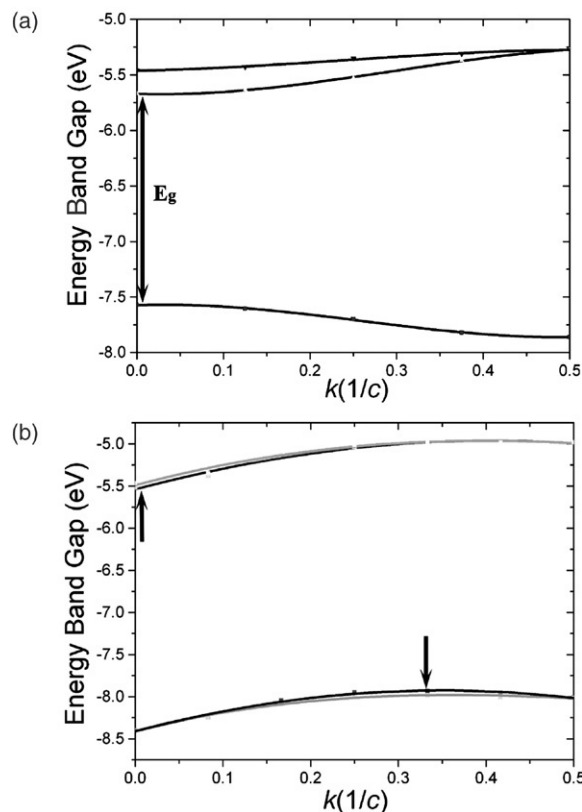


Fig. 4. (a) Electronic band structure of the TiO_2 A-nanotube of diameter 0.8 nm. The minimum direct band gap (EG) of 1.90 eV occurs at $k = 0$ in the reciprocal space. (b) Electronic band structure of the TiO_2 B-nanotube of diameter 1.69 nm. The indirect band gap of 2.44 eV occurs between $k = 0$ and $k = 1/3c$ as indicated by the two arrows in the figure.

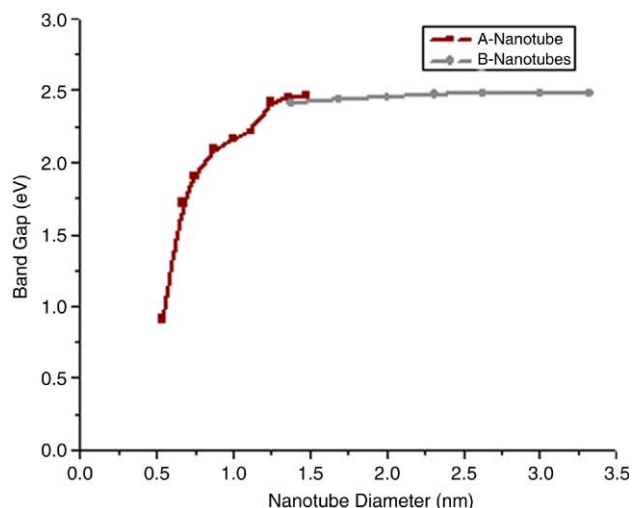


Fig. 5. Relationship between the electronic band gap and the tubule diameters for the A-nanotube and B-nanotube, respectively.

matter of fact, the band gap of the A-nanotube begins to decrease drastically from the diameter of 1.2 nm. As the diameter of the A-nanotube decreases further from 1.2 nm to 0.5 nm, the band gap is reduced by up to 60% to become 0.86 eV. Thus by engineering the diameter of the TiO₂ nanotubes, the band gap can be controlled and tuned to a value that produces a TiO₂ material able to absorb the visible spectrum of solar energy. On the other hand, this controllability is not available to the B-nanotube due to its diameter limit. When the diameter of the TiO₂ nanotubes is larger than 1.3 nm, the band gaps of both A-nanotubes and B-nanotubes are very close in value.

4. Conclusions

Two types of TiO₂ nanotube (A-nanotube and B-nanotube) of concentric tubular structure have been proposed based on experimental observations. We found that, energetically, an A-nanotube is more favorable than a B-nanotube of the same diameter. The electronic band gap of both types of TiO₂ nanotubes is proportional to their diameter. For the A-nanotubes, the band gap can be reduced by up to 60% to match the energy value of visible light as the tubule diameter is reduced to subnanometer values. The A-nanotubes have a direct

band gap while the B-nanotubes have an indirect band gap. Successful engineering and controlling of the atomic structure of the A-nanotubes offer a great opportunity to make TiO₂ nanotubes compatible with solar energy in the visible range for photocatalytic applications.

Acknowledgement

We wish to thank Professor Yue Wu for providing the TiO₂ nanotube samples that were used in the TEM study.

References

- [1] S. Iijima, *Nature* 354 (1991) 56.
- [2] N.G. Chopra, R.J. Luyken, K. Cherrey, V.H. Crespi, M.L. Cohen, S.G. Louie, A. Zettl, *Science* 269 (1995) 966.
- [3] R. Tenne, *Prog. Inorg. Chem.* 50 (2001) 269.
- [4] M. Nath, C.N.R. Rao, *J. Amer. Chem. Soc.* 123 (2001) 4841.
- [5] C.N.R. Rao, M. Nath, *Dalton Transactions* 1 (2003) 1.
- [6] P. Hoyer, *Langmuir* 12 (1996) 1411.
- [7] F. Krumeich, H.-J. Muhr, M. Niederberger, F. Bieri, B. Schnyder, R. Nesper, *J. Amer. Chem. Soc.* 121 (1999) 8324.
- [8] A. Fujishima, T.N. Rao, D.A. Tryk, *J. Photochem. Photobio. C* 1 (2000) 1.
- [9] R. Asahi, Y. Taga, W. Mannstadt, A.J. Freeman, *Phys. Rev. B* 61 (2000) 7459.
- [10] M. Adachi, Y. Murata, I. Okada, S. Yoshikawa, *J. Electrochem. Soc.* 150 (2003) G488.
- [11] S.H. Oh, R.R. Finones, C. Daraio, L.H. Chen, S.H. Jin, *Biomaterials* 26 (2005) 4938.
- [12] S.Q. Liu, A.C. Chen, *Langmuir* 21 (2005) 8409.
- [13] A. Fujishima, K. Honda, *Nature* 37 (1972) 238.
- [14] T. Kasuga, M. Hiramatsu, M. Hirano, A. Hoson, *J. Mater. Res.* 12 (1997) 607.
- [15] G. Dagan, M. Tomkiewicz, *J. Phys. Chem.* 97 (1993) 12651.
- [16] H. Tang, H. Berger, P.E. Schmid, F. Levy, G. Burri, *Solid State Commun.* 23 (1977) 161.
- [17] A.L. Linsebigler, G. Lu, J.T. Yates, *Chem. Rev.* 95 (1995) 735.
- [18] T. Kasuga, M. Hiramatsu, A. Hoson, T. Sekino, K. Niihara, *Adv. Mater.* 11 (1999) 1307.
- [19] A.K. Rappe, C.J. Casewit, K.S. Colwell, W.A. Goddard, W.M. Skiff, *J. Amer. Chem. Soc.* 114 (1992) 10024.
- [20] P. Hohenberg, W. Kohn, *Phys. Rev.* 136 (1964) B864.
- [21] W. Kohn, L.J. Sham, *Phys. Rev.* 140 (1965) A1143.
- [22] J.P. Perdew, Y. Wang, *Phys. Rev. B* 45 (1992) 13244.
- [23] J.K. Burdett, G.J. Hughbanks, G.J. Miller, J.W. Richardson, J.V. Smith, *J. Amer. Chem. Soc.* 109 (1987) 3639.